Selective triggering of phase change in dielectrics by femtosecond pulse trains based on electron dynamics control*

Xu Chuan-Cai(徐传彩), Jiang Lan(姜 澜)†, Leng Ni(冷 妮), and Liu Peng-Jun(刘鹏军)

Laser Micro/Nano-Fabrication Laboratory, School of Mechanical Engineering, Beijing Institute of Technology, Beijing 100081, *China*

(Received 7 August 2012; revised manuscript received 25 September 2012)

In this study we experimentally reveal that the phase change mechanism can be selectively triggered by shaping femtosecond pulse trains based on electron dynamics control (EDC), including manipulation of excitations, ionizations, densities, and temperatures of electrons. By designing the pulse energy distribution to adjust the absorptions, excitations, ionizations, and recombinations of electrons, the dominant phase change mechanism experiences transition from nonthermal to thermal process. This phenomenon is observed in quadruple, triple, and double pulses per train ablation of fused silica separately. This opens up possibilities for controlling phase change mechanisms by EDC, which is of great significance in laser processing of dielectrics and fabrication of integrated nano- and micro-optical devices.

Keywords: phase change, electron dynamics, pulse shaping

PACS: 52.38.Mf, 64.70.kj, 78.20.Jq **DOI:** 10.1088/1674-1056/22/4/045203

1. Introduction

Femtosecond laser interaction with material, especially with dielectrics, has aroused increasing interest, and is considered to be a powerful and promising micromachining technique for ionization of most solid material with greatly reduced recasts, microcracks, and heat-affected zones.[1–3] In addition to the direct ablation,[4,5] confined ablation[6,7] and water-assisted ablation[8,9] have also been investigated. A large number of studies on laser ablation structures[4,8,9] as well as phenomena[10,11] in the ablation process and the effects of different processing parameters[12–14] have been reported. During femtosecond laser ablation of the dielectric, the competing phase change mechanism including the thermal process (nonequilibrium thermal vaporization and melting) and nonthermal process (the Coulomb explosion and electrostatic ablation), may coexist and/or transition to each other in material removal.[15] It is generally considered to be a nonthermal process during the ultrashort laser ablation due to the nonlinear effect and short time scale. However, several studies on dielectric ablation indicate the opposite scenario.[16–19] The existence of a molten zone is demonstrated, which can account for the formation of rims around femtosecond laser ablated craters on dielectrics.[16,17] The protuberance structure on a dielectric surface is proposed to be a consequence of the laser-induced thermal process.[19] The relative role of each phase change mechanism has been intensively debated,[16,18–25] which remains a challenge.

Compared with a long pulse, a femtosecond pulse in some aspects fundamentally changes laser-material interaction mechanism. A femtosecond duration is shorter than or the same as many physical/chemical characteristic times, such as the electron–phonon relaxation time (a few to hundreds of picoseconds) and electron relaxation time (a few to hundreds of femtoseconds), which makes it possible to manipulate/adjust/interfere with electron dynamics.[26–30] Hence, temporally shaped femtosecond laser pulses with pulse delays on a femtosecond time scale allow the exploitation of the electron dynamics control (EDC), which in turn realizes the selective triggering of phase change mechanism to modify structuring processes. The feasibility of EDC by shaping femtosecond pulse trains has been theoretically validated by us.[31,32] Also, in our previous experiments, up to 56 times enhancement in material removal rate and 3 times increase in maximum drilling depth were obtained by pulse train EDC compared with conventional femtosecond laser drilling at the same processing window.[33]

In this study, a detailed investigation is performed in exploring the phase change mechanism by designing pulse energy distribution for EDC during the pulse train processing of fused silica. A femtosecond pulse train with a pulse delay shorter than 1 ps makes the transient localized EDC possible. It is demonstrated by shaping femtosecond pulse trains that (i) the excitations, ionizations, densities, and temperatures of electrons can be modified, (ii) the corresponding material optical and thermal properties can be changed, and hence, (iii) the phase change mechanism can be selectively triggered.

2. Experimental setup

The experimental setup includes a 35-fs, 800-nm Ti: sapphire laser system and a pulse shaper (BSI MIIPS BOX 640)

*Project supported by the National Basic Research Program of China (Grant No. 2011CB013000) and the National Natural Science Foundation of China (Grant Nos. 90923039 and 51025521).

†Corresponding author. E-mail: jianglan@bit.edu.cn

© 2013 Chinese Physical Society and IOP Publishing Ltd

system. The time delay (300 fs in this study) and pulse distribution are shaped in the temporal domain by the pulse shaper. All the subpulses have identical pulse duration and frequency chirp. Methods to be embedded in the pulse shaper and cross correlation are used to monitor the pulse trains as shown in Fig. 1. A half-wave plate combined with a polarizer is used for continuous energy adjustment. The total fluence per train used in our experiment is 12 J/cm^2. The shaped pulses are focused by a 20× objective lens (N.A. = 0.45, Olympus) onto the front surface of fused silica (0.5-mm thickness), which is driven by a computer controlled 6-DOF nanomanipulation stage. The surface of the sample is positioned normally to the direction of the incident laser beam in air at atmospheric pressure and temperature. A scanning electron microscope (SEM) and an atomic force microscope (AFM) are used to characterize the ablation sizes and surface morphologies.

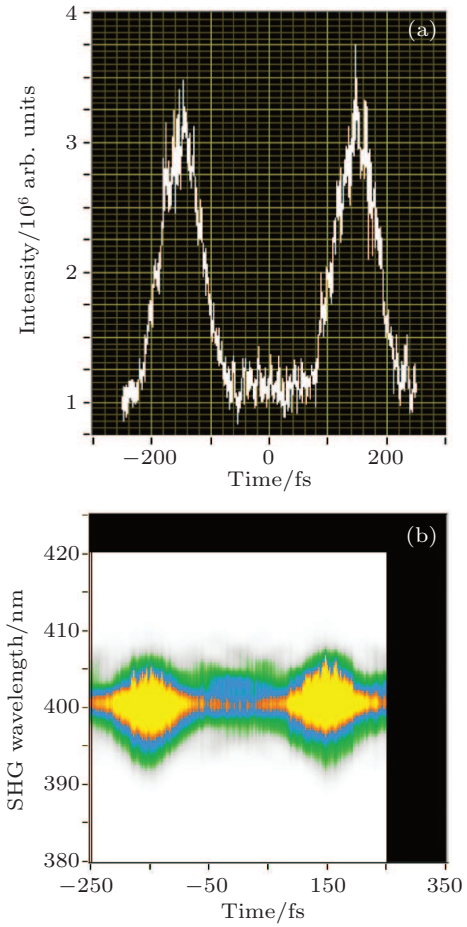


Fig. 1. (color online) Measured pictures of a shaped pulse train consisting of two identical subpulses.

3. Results and discussion

The phase change mechanism is determined by the ablated surface structure in this study. In order to gain an insight into the modification factor, a single burst instead of multiple bursts is used. Figure 2 shows the ablated structures of fused silica by a single quadruple-pulse train excitation at the pulse energy distributions of 4:3:2:1 and 1:2:3:4 respectively. The corresponding diameters, depths, and recast heights of the ablated structures are measured by an AFM as shown in Fig. 3. It can be seen that both the ablation diameter and depth of the structure produced by an increasing energy distribution are smaller but with a larger recast height.

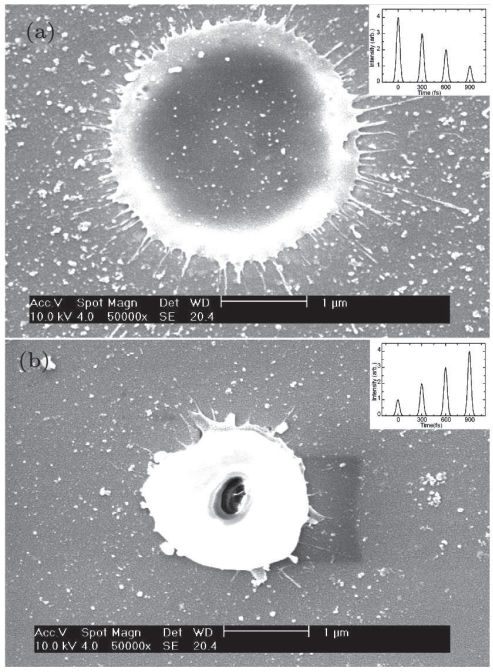


Fig. 2. SEM images of surface ablated by a single quadruple-pulse train designed to trigger the phase change mechanism selectively through EDC. The energy distributions are (a) 4:3:2:1 and (b) 1:2:3:4. The corresponding pulse train is shown in the inset.

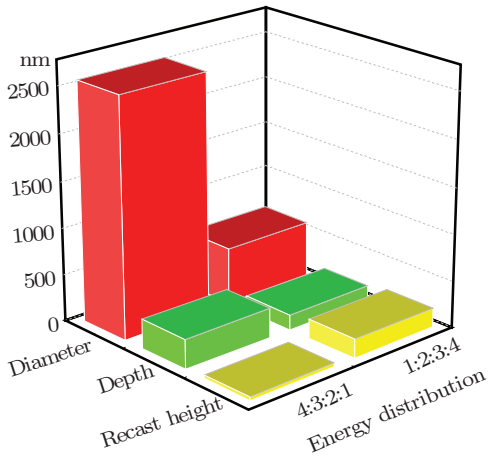


Fig. 3. (color online) Energy distribution dependences of diameter, depth, and recast height of the ablation structure on the surface of fused silica.

In the case of 4:3:2:1, the fluences of the first two subpulses are above the ablation threshold, and the fluences of the subsequent two subpulses are below the threshold energy. A high electron density created by strong subpulses can be further increased by the subsequent weak subpulses. Because the pulse delay is on the time scale of the electronic decay of fused silica, some electrons excited by the former subpulse are still in the conduction band before the next subpulse irradiates,

which leads to more seed-free electrons and contributes to the enhancement of avalanche ionization. In addition, the pulse train technology prolongs the energy absorption time and prevents electrons from overheating.[31] Therefore, the nonthermal phase change mechanisms, including Coulomb explosion and electrostatic ablation, are the main phase change mechanisms when the pulse energy distribution is 4:3:2:1, which will take heat away by the removed debris. Thus the thermal phase change mechanisms are inhibited due to less heat accumulation.

However, in the case of 1:2:3:4, the initial weak subpulses are not intense enough for efficient multiphoton ionization (MPI). In addition, the recombination results in less free electrons. Due to the absence of seed electrons, when the subsequent subpulses irradiate, an increase of the free electron density by avalanche ionization (AI) is not operative. Hence, the final electron density is not sufficient for the effectiveness of the Coulomb explosion or electrostatic ablation. On the other hand, the ineffective nonthermal ablation contributes to the heat accumulation in the process, owing to the fact that the delay between two subpulses is 300 fs. On this time scale, the heat generated by the former subpulse interaction with the fused silica still has not dissipated when the next subpulse irradiates.[17] Then the focal area is heated to a high temperature when the stronger subsequent subpulses irradiate the sample, which enhances the thermal ablation. A localized melting of the fused silica results from an accumulation of thermal energy.[18] The recast is formed due to the generation of a molten layer in the ablation process.[16,17,19]

Therefore, during femtosecond laser ablation of fused silica, the nonthermal processes (Coulomb explosion and electrostatic ablation) are mainly triggered when the energy distribution is 4:3:2:1. While the thermal process, such as melting, becomes the main phase change mechanism when the pulse energy distribution is 1:2:3:4.

The detailed ablation process related to the phase change mechanism is investigated by a femtosecond pulse train with less subpulses. A single triple-pulse train ablation of fused silica is shown in Fig. 4. As shown in Fig. 4(a), the inner surface of the ablated structure is clean in appearance at the energy distribution of 3:1:1. In this case, the nonthermal phase change mechanism comes into play, which is similar to that in Fig. 2(a), with a larger ablation size due to a higher electron density resulting from the relatively concentrated energy distribution. When the pulse energy distribution is reversed, the ablated structure shows a scaly surface, indicating a resolidified splash of a molten layer generated in the ablation process as shown in Fig. 4(b). A three-layer structure, indicated by arrows in the figure, corresponding to three subpulses, is formed. When the first weak subpulse with energy around the breakdown threshold irradiates, by which critical electron density is produced due to the MPI and AI, a shallow crater with clean surface is obtained, owing to the Coulomb explosion and electrostatic ablation. Then when the second subpulse with the same energy reaches the surface, the free electrons still in the conduction band will contribute to the AI. Moreover, stronger ablation occurs because the melting coexists with the Coulomb explosion and electrostatic ablation. This is due to the reheating of the electrons produced by the first subpulse, which leads to the heat accumulation. Finally, when the last strong subpulse reaches the focal area, the thermal phase change mechanism becomes dominant and leads to the formation of the recast, which is similar to the case in Fig. 2(b).

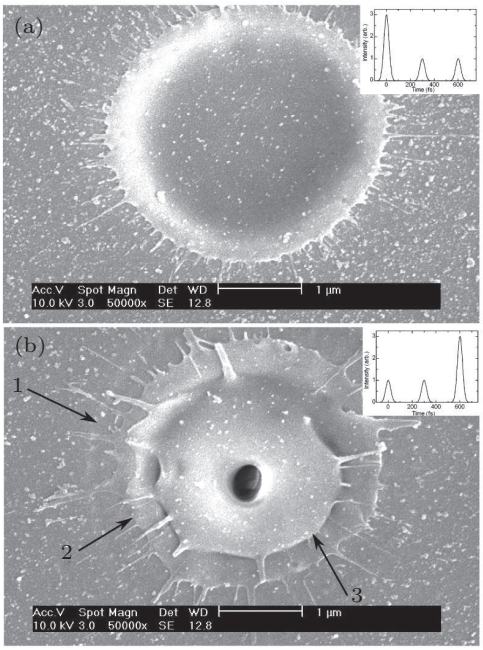


Fig. 4. SEM images of surface ablated by a single triple-pulse train designed to trigger the phase change mechanism selectively through EDC. The energy distributions are (a) 3:1:1 and (b) 1:1:3. The corresponding pulse train is shown in the inset.

By designing the pulse energy distribution based on electron dynamics, the phase change mechanism can also be selectively triggered by a double-pulse train. As a result, the morphology of the structure can be controlled [Figs. 4(a)–4(c)]. When the energy of the two subpulses is adjusted to be above the threshold, a scaly surface is observed as shown in Fig. 5(a). High electron mobility induced by the first subpulse enhances electron screening. Electron screening reduces the accumulation of positive charges during a femtosecond laser pulse, and thus reduces the electric field, which weakens the effectiveness of the Coulomb explosion. The rough surface indicates that the thermal vaporization dominates the phase change mechanism during the irradiation of the second subpulse. At the same total fluence, when the energy of the first subpulse is adjusted to be slightly above the threshold, the Coulomb explosion dominates the material removal process[15,20,34] during the first subpulse and melting comes into play during the second subpulse as shown in Fig. 5(b). When the pulse energy distribution is reversed, the clean surface as shown in Fig. 5(c), indicates that the gentle ablation by the Coulomb explosion is

the main phase change mechanism. Figures 5(c1) and 5(c2) show the good repeatability of the results.

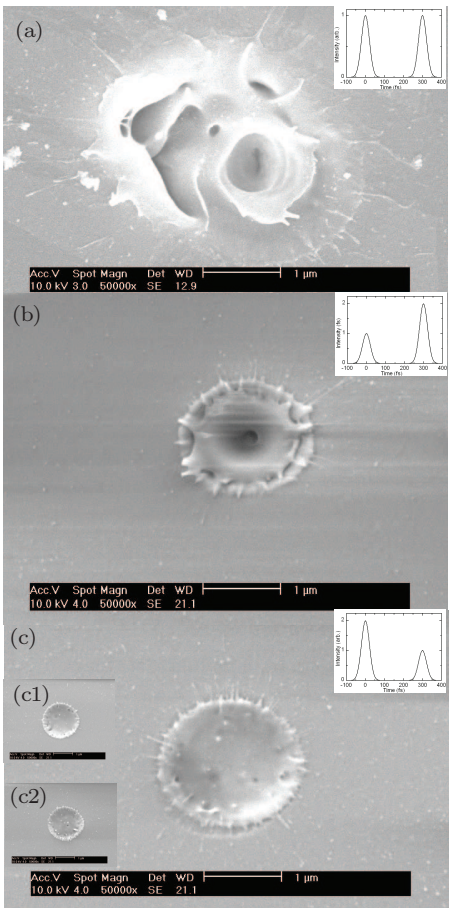


Fig. 5. SEM images of surface ablated by a single double-pulse train designed to trigger the phase change mechanism selectively through EDC. The energy distributions are (a) 1:1, (b) 1:2, and (c)–(c2) 2:1. The corresponding pulse train is shown in the inset.

4. Conclusions

Based on the EDC, the phase change mechanism is selectively triggered by designing the pulse energy distribution of subpulses in a train with the pulse delay on a femtosecond time scale. It is demonstrated that the transition between the nonthermal and thermal phase change mechanisms can be achieved by the EDC. By properly adjusting the electron dynamics during pulse train ablation with a decreasing subpulse energy distribution, the nonthermal phase change mechanism dominates the process. In contrast, when the energy distribution is reversed, the thermal phase change mechanism is dominant. The surface morphology of the ablated structure can be modified by adjusting the subpulse energy distribution to change the transient localized electron dynamics, which in turn triggers the corresponding phase change mechanism. This is validated by the experiments with different numbers of subpulses in a femtosecond pulse train.

References

[1] Kawata S, Sun H B, Tanaka T and Takada K 2001 *Nature* **412** 697
[2] Gattass R R and Mazur E 2008 *Nat. Photon.* **2** 219
[3] Jiang L and Tsai H L 2005 *Appl. Phys. Lett.* **87** 151104
[4] Sun H Y, Luo F F, He F, Liao Y and Xu J 2010 *Chin. Phys. B* **19** 054210
[5] Zhong M J, Guo G L, Yang J Y, Ma N H, Ye G, Guo X D, Li R X and Ma H L 2008 *Chin. Phys. B* **17** 1223
[6] Zheng Z Y, Zhang J, Lu X, Hao Z Q, Xu M H, Wang Z H and Wei Z Y 2005 *Chin. Phys. Lett.* **22** 1725
[7] Zheng Z Y, Zhang J, Hao Z Q, Yuan X H, Zhang Z, Lu X, Wang Z H and Wei Z Y 2006 *Chin. Phys.* **15** 580
[8] An R, Li Y, Dou Y P, Fang Y, Yang H and Gong Q H 2004 *Chin. Phys. Lett.* **21** 2465
[9] Li Y and Qu S L 2012 *Chin. Phys. B* **21** 034208
[10] Li Z H, Zhang D M, Yu B M and Guan L 2002 *Chin. Phys. Lett.* **19** 1841
[11] Dai Y, Yu G J, Wu G R, Ma H L, Yan X N and Ma G H 2012 *Chin. Phys. B* **21** 025201
[12] Fang R R, Zhang D M, Wei H, Li Z H, Yang F X and Tan X Y 2008 *Chin. Phys. Lett.* **25** 3716
[13] Bian F, Wang R, Yang H X, Zhang X Z, Li J Q, Xu H X, Xu J J and Zhao J M 2010 *Chin. Phys. Lett.* **27** 088101
[14] Han W, Wang F, Zhou L D, Feng B, Jia H T, Li K Y, Xiang Y and Zheng W G 2012 *Chin. Phys. B* **21** 077901
[15] Stoian R, Ashkenasi D, Rosenfeld A and Campbell E 2000 *Phys. Rev. B* **62** 13167
[16] Ben-Yakar A, Byer R L, Harkin A, Ashmore J, Stone H A, Shen M and Mazur E 2003 *Appl. Phys. Lett.* **83** 3030
[17] Ben-Yakar A, Harkin A, Ashmore J, Byer R L and Stone H A 2007 *J. Phys. D* **40** 1447
[18] Schaffer C B, García J F and Mazur E 2003 *Appl. Phys. A* **76** 351
[19] Teng Y, Zhou J J, Luo F F, Ma Z J, Lin G and Qiu J R 2010 *Opt. Lett.* **35** 2299
[20] Stoian R, Rosenfeld A, Ashkenasi D, Hertel I, Bulgakova N and Campbell E 2002 *Phys. Rev. Lett.* **88** 97603
[21] Chimier B, Uteza O, Sanner N, Sentis M, Itina T, Lassonde P, Legare F, Vidal F and Kieffer J C 2011 *Phys. Rev. B* **84** 094104
[22] Han J H, Feng G Y, Yang L M, Zhang Q H, Fu Y Q, Niu R H, Zhu Q H, Xie X D and Zhou S H 2011 *Acta Phys. Sin.* **60** 028106 (in Chinese)
[23] Rublack T, Hartnauer S, Kappe P, Swiatkowski C and Seifert G 2011 *Appl. Phys. A* **103** 43
[24] Stuart B C, Feit M D, Herman S, Rubenchik A M, Shore B W and Perry M D 1996 *J. Opt. Soc. Am. B* **13** 459
[25] Stuart B C, Feit M D, Herman S, Rubenchik A M, Shore B W and Perry M D 1996 *Phys. Rev. B* **53** 1749
[26] Sansone G, Benedetti E, Calegari F, Vozzi C, Avaldi L, Flammini R, Poletto L, Villoresi P, Altucci C, Velotta R, Stagira S, De Silvestri S and Nisoli M 2006 *Science* **314** 443
[27] Cavalieri A L, Müller N, Uphues T, Yakovlev V S, Baltuška A, Horvath B, Schmidt B, Blümel L, Holzwarth R and Hendel S 2007 *Nature* **449** 1029
[28] Goulielmakis E, Yakovlev V S, Cavalieri A L, Uiberacker M, Pervak V, Apolonski A, Kienberger R, Kleineberg U and Krausz F 2007 *Science* **317** 769
[29] Meckel M, Comtois D, Zeidler D, Staudte A, Pavicic D, Bandulet H C, Pepin H, Kieffer J C, Dorner R, Villeneuve D M and Corkum P B 2008 *Science* **320** 1478
[30] Goulielmakis E, Schultze M, Hofstetter M, Yakovlev V S, Gagnon J, Uiberacker M, Aquila A L, Gullikson E M, Attwood D T, Kienberger R, Krausz F and Kleineberg U 2008 *Science* **320** 1614
[31] Wang C, Jiang L, Wang F, Li X, Yuan Y P and Tsai H L 2011 *Phys. Lett. A* **375** 3200
[32] Wang C, Jiang L, Wang F, Li X, Yuan Y P, Tsai H L and Lu Y F 2012 *J. Phys.: Condens. Matter* **24** 275801
[33] Jiang L, Liu P J, Yan X L, Leng N, Xu C C, Xiao H and Lu Y F 2012 *Opt. Lett.* **37** 2781
[34] Mijoule V, Lewis L J and Meunier M 2006 *Phys. Rev. A* **73** 033203